PHYSICAL REVIEW C VOLUME 17, NUMBER 2 FEBRUARY 1978

Decay of $^{143}Gd^{m+g}$ by positron emission and electron capture*

R. B. Firestone, R. A. Warner, and Wm. C. McHarris
Department of Chemistry, Cyclotron Laboratory, and Department of Physics

W. H. Kelly
Cyclotron Laboratory and Department of Physics, Michigan State University, East Lansing, Michigan 48824
(Received 3 August 1977)

In this study the decay of $^{143}Gd^{g+m}$ by positron emission and electron capture and the isomeric decay of $^{143}Eu^{m}$ were investigated. γ rays associated with $^{143}Gd^{g+m}$ were placed on the basis of excitation functions, half-life, and γ-γ coincidence information. We assigned 61 γ rays deexciting 33 levels in ^{143}Eu from the decay of 112 ± 2 sec $^{143}Gd^{m}$. Another 7 γ rays deexcite an additional 6 levels in ^{143}Eu from 39 ± 2 sec $^{143}Gd^{g}$ decay. A small delayed p or α branch associated with ^{143}Gd decay was observed with an upper limit of 1×10^{-5}. The half-life of the $^{143}Eu^{m}$ isomer at 389.47 keV was found to be 50.0 ± 0.5 μ sec. The resulting level structure observed in ^{143}Eu is explained quite satisfactorily in terms of a triaxial weak-coupling model.

RADIOACTIVITY $^{143}Gd^{g+m}$, $^{143}Eu^{m}$, measured $T_{1/2}$, delayed $p+\alpha$, E_γ, I_γ, $\gamma\gamma$ coin, $\sigma(E)$; deduced logft, Q. ^{143}Eu deduced levels, J, π.

NUCLEAR STRUCTURE ^{143}Eu; calculated levels, J, π. Triaxial weak-coupling model.

I. INTRODUCTION

The decay of $^{143}Gd^{g+m}$ continues our studies of odd-mass N=79 nuclei, which have included $^{137}Ce^{g+m}$,[1] $^{139}Nd^{g+m}$,[2] and $^{141}Sm^{g+m}$.[3,4] The first studies of $^{143}Gd^{m}$ decay were reported by J. van Klinken et al.,[5] who presented a modest decay scheme; later studies, by Wisshak et al.,[6] presented a more thorough decay scheme. In this work we have nearly doubled the known information about $^{143}Gd^{m}$ decay and present our new data concerning $^{143}Gd^{g}$ decay. We had previously reported a half-life measurement of $^{143}Gd^{g+m}$;[7] here we present our total decay scheme data in more detail. The level structure in ^{143}Eu was discussed by Wisshak et al. in terms of a generalized decoupling model, which gave only fair agreement with experiment. In this paper we shall show that a good qualitative agreement with experiment can be attained using a weak-coupling model.

II. SOURCE PREPARATION

$^{143}Gd^{g+m}$ were produced by the ^{144}Sm(^{3}He,4n)^{143}Gd reaction with a 50-MeV ^{3}He beam produced by the Michigan State University sector-focused cyclotron. Enriched targets of $^{144}Sm_2O_3$ (95.10% ^{144}Sm, obtained from the Isotopes Division, Oak Ridge National Laboratory) were bombarded in the terminal of a He-jet recoil transport system, which is described elsewhere.[7]

The primary impurities encountered in these studies were ^{140}Pm ($t_{1/2}$ = 5.8 min), $^{141}Sm^{m}$ ($t_{1/2}$ = 22.7 min), ^{142}Eu ($t_{1/2}$ = 1.2 min), ^{144}Eu ($t_{1/2}$ = 10.5 sec), ^{14}O ($t_{1/2}$ = 70.5 sec), ^{16}N ($t_{1/2}$ = 7.11 sec), ^{10}C ($t_{1/2}$ = 19.4 sec), and the ^{143}Eu daughter activity ($t_{1/2}$ = 2.61 min). None of these impurities was both intense and complex enough to hinder the studies of interest seriously, and all were already well understood. Coincidence and half-life experiments were employed to delineate the transitions of interest further.

III. γ-RAY SPECTRA

A. Singles spectra

$^{143}Gd^{g+m}$ singles spectra were taken with an 18.0% efficient Ge(Li) detector (relative to a 7.6×7.6-cm NaI(Tl) detector at 25 cm for the 1332-keV ^{60}Co photopeak). The resolution of this detector was 2.1 keV full width at half maximum at 1332 keV. Activity was collected on a slowly moving paper tape at a point shielded from the detector and counted during the interval from 10 sec to 90 sec after bombardment. A spectrum collected in this manner is shown in Fig. 1.

Seven γ rays were assigned to $^{143}Gd^{g}$ decay and 61 γ rays were assigned to $^{143}Gd^{m}$ decay; these are listed in Table I. Assignments were made on the basis of half-life, excitation functions, and coincidence information (discussed below), and virtually all of the observed activity could be assigned either to $^{143}Gd^{g+m}$ or to the appropriate known impurity. Precise energy calibrations were performed using ^{56}Co, $^{110}Ag^{m}$, ^{152}Eu, ^{182}Ta, and ^{226}Ra internal standards, and the quoted errors reflect the statistical scatter in these measurements. Certain transitions were apparent only in the coincidence studies, and greater errors are reflected in these energy and intensity assignments.

The paper of Wisshak et al.[6] included

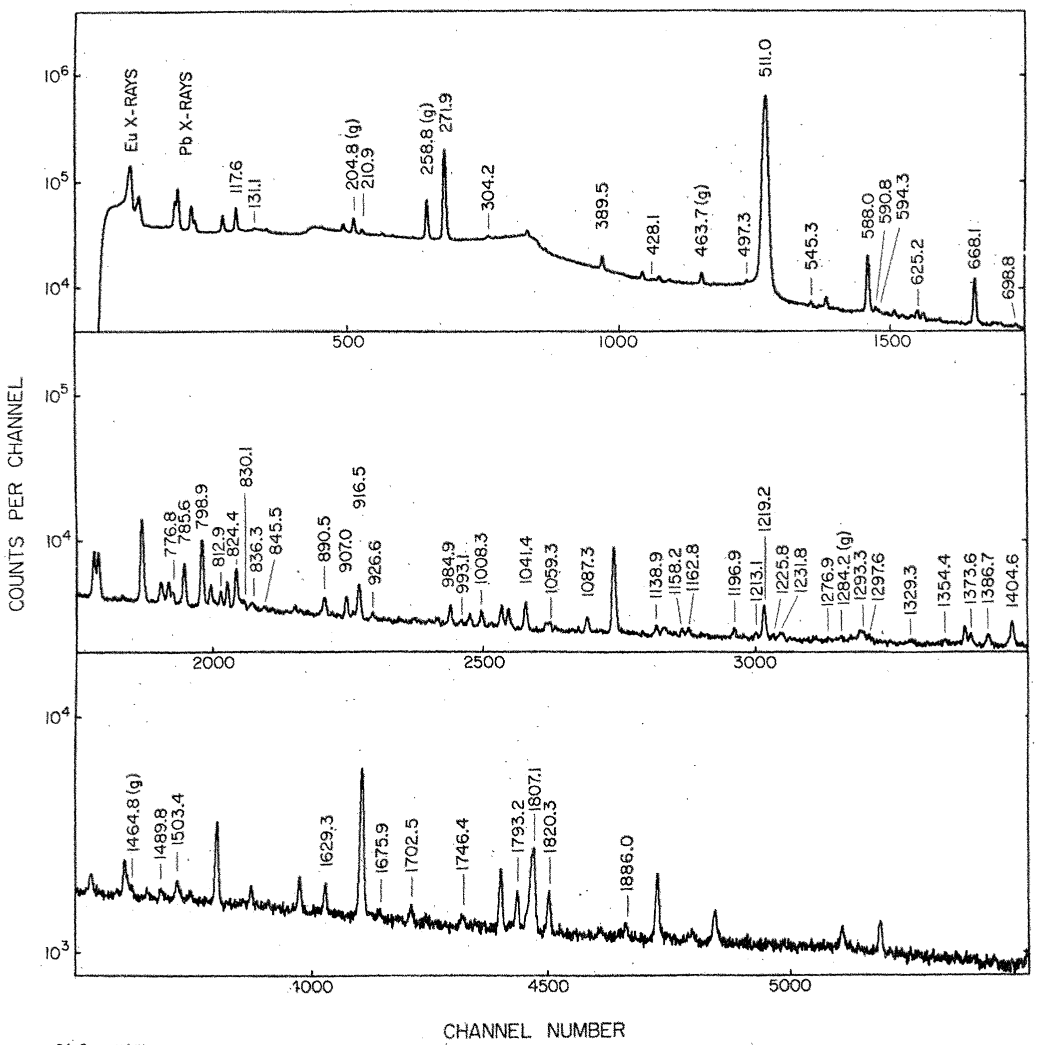

FIG. 1. $^{143}Gd^{g+m}$ γ-ray spectrum produced by the $^{144}Sm(^3He,4n)^{143}Gd$ reaction using a 50-MeV ^3He beam. Only transitions assigned to $^{143}Gd^{g+m}$ are identified here, however, all observed transitions were assigned to their appropriate decays.

conversion-electron data obtained utilizing a mini-orange spectrometer. We utilize these data in the following discussions and have included multipolarities determined from combining them with our γ-ray data in Table I.

B. Excitation functions

An additional useful method for sorting the ^{143}Gd transitions from the contaminants was through excitation functions. Many impurities were recognized easily in this manner, and weak transitions could sometimes be identified in this way when half-life measurements were impossible. Spectra were recorded for beam energies from 31- to 76-MeV provided by degrading a 76-MeV ^3He incident beam with an automatically adjustable absorber unit.[7] Representative relative cross-section plots for the production of $^{143}Gd^{m+g}$ and various impurities are shown in Fig. 2. The absolute normalizations of these excitation functions were not measured; however, this was not necessary for identification of the various nuclides.

C. Half-life determinations

The half-life of $^{143}Gd^m$ was determined by following the net peak areas of the 271.94-, 588.00-, and 798.89-keV γ rays as a function of time. The $^{143}Gd^g$ half-life was similarly measured by following the 258.81-keV peak area. A series of six consecutive 90-sec spectra were recorded, as well as a separate series of six consecutive 15-sec spectra. A constant-rate pulser peak was included for dead-time correction. The sequencing system for advancing the new thermalizer sources, disposing of the old activity sequentially, and routing the spectra to the computer is described elsewhere.[7] After the background subtraction and dead-time corrections, the half-life points were least-squared fit with straight lines (using a second-order

TABLE I. Energies and relative intensities of γ rays from the decays of $^{143}Gd^{m+g}$.

Energy (keV)[a]	Intensity[b]	Energy (keV)[a]	Intensity[b]
$^{143}Gd^{m}$			
117.57±0.05 (*M*2)	7.7 ±0.6	1059.3 ±0.1	1.0 ±0.1
131.1 ±0.1	0.44±0.07	1087.3 ±0.1	1.9 ±0.2
210.9 ±0.1 (*M*1)	1.3 ±0.1	1138.9 ±0.1	0.96±0.09
271.94±0.03 (*M*1)	≡100	1158.2 ±0.1	0.66±0.09
304.2 ±0.1 (*M*1,*E*2)	1.2 ±0.1	1162.8 ±0.2	0.9 ±0.10
389.47±0.05 (*E*3)	4.1 ±0.3	1196.9 ±0.1	1.06±0.09
428.1 ±0.2	0.3 ±0.1	1213.1 ±0.3	0.66±0.09
497.3 ±0.1	0.7 ±0.1	1219.21±0.07	4.9 ±0.4
545.3 ±0.1	0.7 ±0.1	1225.8 ±0.5	0.3 ±0.1
588.00±0.03 (*M*1,*E*2)	18.6 ±1.3	1231.8 ±0.3	0.8 ±0.1
590.8 ±0.2	0.4 ±0.2	1276.9 ±0.5	0.3 ±0.1
594.3 ±0.1	0.69±0.06	1293.3 ±0.2	1.0 ±0.1
625.23±0.08	1.4 ±0.1	1297.6 ±0.2	0.42±0.07
668.10±0.03 (*M*1,*E*2)	11.5 ±0.8	1329.3 ±0.5	0.3 ±0.1
698.8 ±0.1	0.45±0.06	1354.4 ±0.2	0.6 ±0.1
776.8 ±0.1 (*M*1,*E*3)	1.0 ±0.1	1373.6 ±0.1	1.3 ±0.1
785.56±0.06 (*E*2)	6.5 ±0.5	1386.69±0.07	1.5 ±0.1
798.89±0.06 (*E*2)	12.7 ±0.9	1404.56±0.07	3.4 ±0.3
824.43±0.09 (*E*2)	5.9 ±0.4	1489.8 ±0.2	0.78±0.09
830.1 ±0.1	0.64±0.06	1503.4 ±0.1	1.4 ±0.1
836.3 ±0.1	0.66±0.06	1629.3 ±0.1	2.3 ±0.2
845.5 ±0.2	0.3 ±0.1	1633.3 ±0.6	0.10±0.05
890.52±0.09 (*M*1,*E*2)	2.1 ±0.2	1675.9 ±0.3	0.57±0.09
906.96±0.06 (*E*2)	2.5 ±0.3	1702.5 ±0.1	1.3 ±0.1
916.53±0.05 (*E*2)	5.1 ±0.4	1746.4 ±0.1	0.9 ±0.1
926.6 ±0.2	0.65±0.09	1793.21±0.07	3.1 ±0.2
984.93±0.05 (*M*2,*E*3)	2.4 ±0.2	1807.14±0.07	9.1 ±0.7
993.1 ±0.3	0.55±0.06	1820.27±0.07	3.6 ±0.3
1008.28±0.05 (*M*1,*E*3)	1.6 ±0.1	1886.0 ±0.2	0.9 ±0.1
1041.35±0.05	3.6 ±0.3	2338.9 ±0.8	0.3 ±0.1
$^{143}Gd^{g}$			
204.77±0.05	25.9 ±1.9		
258.81±0.03 (*M*1,*E*3)	≡100		
463.7 ±0.1	13.2 ±1.0		
554.1 ±0.3	1.0 ±0.5		
812.9 ±0.1	7.2 ±0.7		
1284.2 ±0.4	1.4 ±0.5		
1464.8 ±0.4	1.2 ±0.4		

[a]The errors given on the energies reflect both statistical scatter and calibration standard errors.

[b]The errors given on the intensities reflect both statistical scatter and calibration standard errors. Some transitions were observed only in coincidence measurements and yielded less precise intensities.

polynomial). Representative half-life plots are presented in Fig. 3. From an average of such curves we determined the half-life of $^{143}Gd^{m}$ to be 112±2 sec and that of $^{143}Gd^{g}$ to be 39±2 sec. In addition, 30 transitions were assigned to $^{143}Gd^{g+m}$ partially on the basis of half-life.

The half-life of the 389.47-keV state in ^{143}Eu was measured by utilizing fast beam-sweeping techniques. After bombardments of a ^{144}Sm target with 27-MeV protons for intervals of ≈200 μsec, a series of ten 70-μsec spectra were taken. The decay of the 117.57-, 271.94-, and 389.47-keV γ rays from this state were found to yield similar half-lives. The 271.94-keV γ ray was by far the strongest and could be followed through six spectra. Dead-time corrections were determined from a constant-rate pulser peak, and the half-life for the 389.47-keV state was measured to be 50.0±0.5 μsec. A half-life plot of these data is presented in Fig. 4. This experiment will be discussed in greater detail elsewhere.[8]

D. Coincidence spectra

γ-γ megachannel coincidence spectra were taken with 18% and 10% efficient Ge(Li) detectors. Coincidence data pairs were collected sequentially on magnetic tape for off-line sorting with background subtraction. A standard three-parameter ($E_\gamma \times E_\gamma \times t$) fast-slow electronics setup with constant

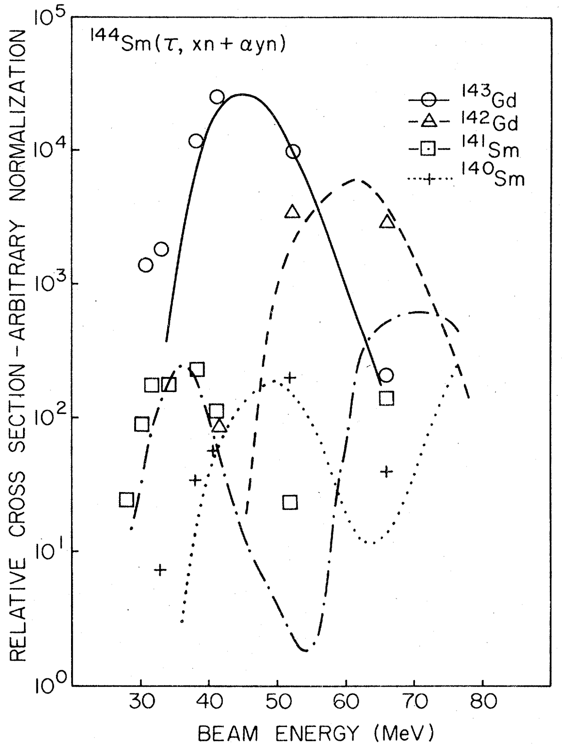

FIG. 2. Experimental excitation function for 30-76-MeV ^{3}He on a ^{144}Sm target. The curves plotted were calculated using the computer code ALICE,[21] although the absolute normalizations are all arbitrary. It is interesting to note the double peak in the ^{141}Sm production cross-section caused by the different Q values for the (^{3}He,$\alpha 2n$) and (^{3}He,$2p4n$) reactions. This is qualitatively predicted by the calculation.

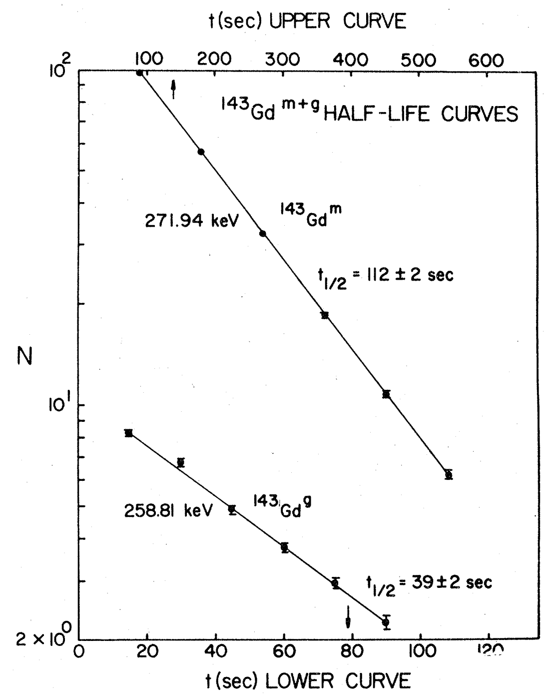

FIG. 3. Half-life plots for the strongest respective transitions in $^{143}Gd^{g+m}$ decays. These data have been corrected for deadtime, and the half-life was extracted from a least-squares fit. The normalization shown is arbitrary.

fraction timing was used.[9] Sample coincidence gates are shown in Fig. 5, along with the corresponding integral coincidence spectra for the X (18%) side. In general, transitions of intensity 0.2% per decay or greater were observable in the coincidence spectra. All transitions reported in this paper were either seen in coincidence with γ rays ascribed to $^{143}Gd^{g+m}$, or were of sufficient intensity to give definite negative coincidence results. Energy sums were used only as correlative evidence to these coincidence results. A summary of the coincidence information is presented in Table II.

E. β-delayed proton spectra

The large amount of available β-decay energy for $^{143}Gd^{m+g}$ allows the possibility of decay to high-lying levels unbound with respect to proton decay. The p separation energy in ^{143}Eu is 2.64 MeV, and, considering the height of the Coulomb barrier, about 2.5 MeV above this we expect p decay to compete more or less equally with γ decay. A delayed p and/or α spectrum was collected using a thin Si surface barrier

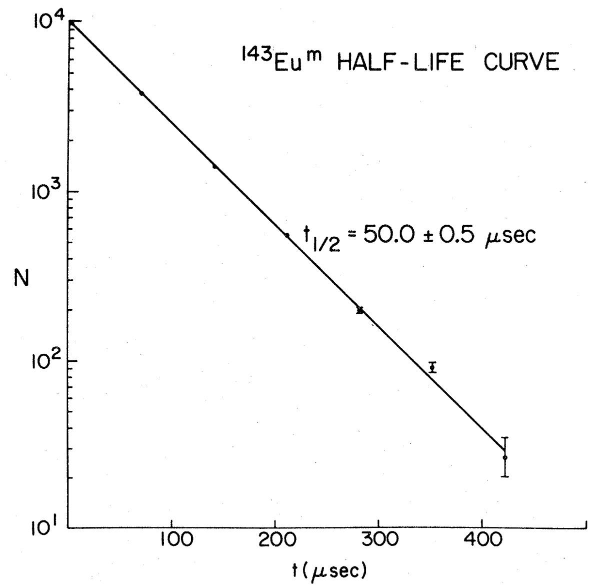

FIG. 4. Half-life plot for the decay of the 389.47-keV state in ^{143}Eu. These data have been corrected for deadtime, and the half-life was extracted from a least-squares fit.

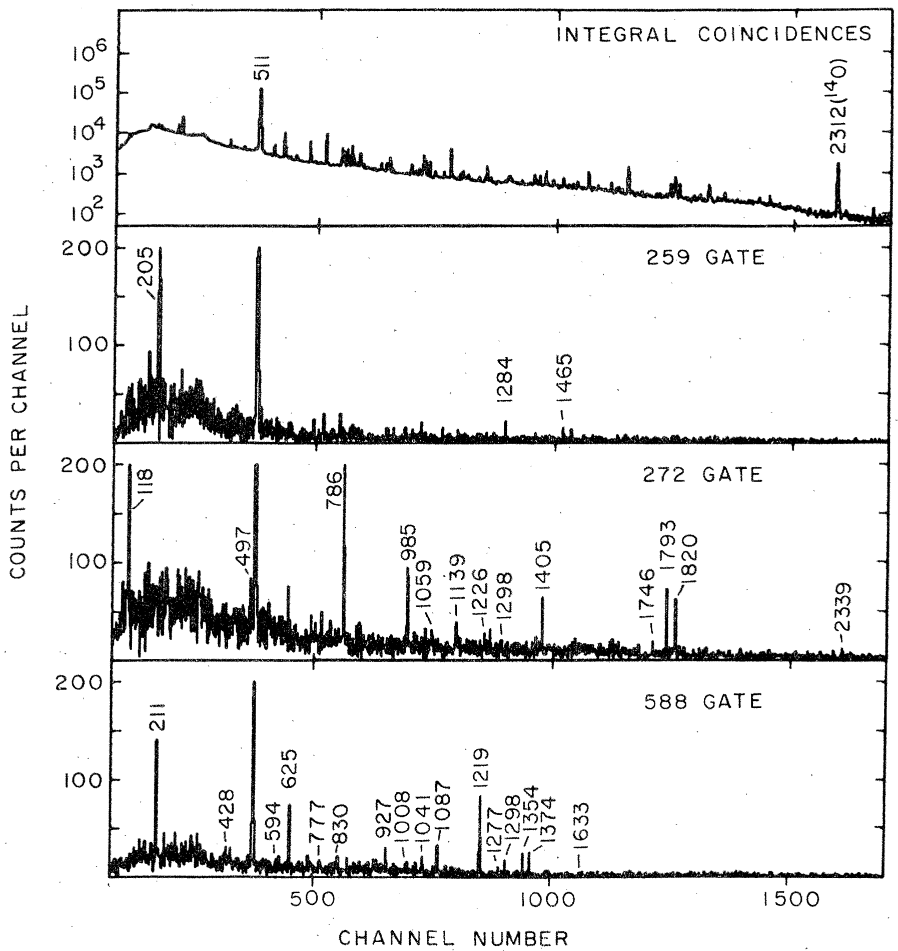

FIG. 5. Representative coincidence data for $^{143}Gd^{g+m}$ decay. All coincidences were confirmed by gates run on both detectors as well as by other interlocking coincidence data.

detector backed by a thicker Si veto detector to eliminate β events. A particle spectrum obtained in this manner is shown in Fig. 6. A broad distribution of p/α energies was observed with very few events below 3 MeV. From these data we could set an upper limit of one part in 10^5 delayed p/α decays per $^{143}Gd^{m+g}$ decay. This result was of importance in eliminating possible strong β-decay branches to very high-lying levels; however, statistics were too poor to make further use of these data for measuring Q_β.

IV. DECAY SCHEMES

A. $^{143}Gd^g$

In Fig. 7 we have constructed a $^{143}Gd^g$ decay scheme from the combination of the coincidence, excitation function, and half-life data. The 204.77-, 258.81-, 463.7-, and 812.9-keV transitions were all observed to have approximately a 39-sec half-life. Intensity balances placed the 258.81-keV γ, and coincidences between this γ ray and the 204.77-, 554.1-, 1284.2-, and 1464.8-keV γ's placed levels at 463.7, 812.9, 1543.0, and 1723.6 keV. No γ rays were observed in coincidence with the strong 463.7- or 812.94-keV γ's, so these were placed as direct ground-state transitions from the states of the same energy. The intensities assigned to each transition are in percent per decay of $^{143}Gd^g$, assuming no second-forbidden direct ground-state β transitions. Logft values were calculated from the compilation by Gove and Martin[11] using the average Q_ε value calculated from the mass excesses reported by Wapstra and Bos.[12]

Systematics suggest $^{143}Gd^g$ has $J^\pi = 1/2^+$ in analogy with both $^{145}Gd^g$ and $^{141}Sm^g$.[10] From a single-particle shell-model picture we expect to observe low lying $\pi s_{1/2}$ and $\pi d_{3/2}$ neutron states in ^{143}Eu, both of which should be fed by $^{143}Gd^g$ decay. The $M1$ transition from the 258.81-keV state to the $\pi d_{5/2}$ ground state allows us to assign spin $3/2^+$ to that state and from shell-model systematics we assign spin $1/2^+$ to the 463.7-keV state. These two states are expected to contain most of the single-particle $d_{3/2}$ and $s_{1/2}$ orbitals, respec-

TABLE II. $^{143}Gd^{m+g}$ coincidence summary.

Gate (keV)[a]	Coincident γ Rays
118	272
205	259
259	205, 554, 1284, 1465
211	588
272	118, 497, 786, 985, 1059, 1139, 1226, 1293, 1405, 1746, 1793, 1820, 2339
304	1503
497	272, 985
545	668
554	259
588	211, 428, 594, 625, 777, 830, 927, 1008, 1041, 1087, 1219, 1277, 1298, 1354, 1374, 1633
594	545, 588, 625
625	588
668	131, 545, 846, 1197
699	1329
777	588
786	272, 836, 1139
799	830, 1008, 1087, 1163
824	1387
830	799
891	917
907	591, 1158
917	891
927	588
985	272, 497
993	588
1008	799
1041	588
1059	272
1087	588, 799
1139	272, 786
1158	907
1163	211, 799
1232	588
1298	588
1329	699
1354	588
1374	588
1387	824
1405	272
1465	259
1490	272
1503	304
1793	272
1820	272

[a]Only gates containing positive coincidence information are included. All gates contained 511-keV $\gamma^{\pm}$ radiation.

tively. From the $\log ft$ values and the γ deexcitation patterns, we can but limit the J^π assignments for the three remaining states to $1/2^+$ or $3/2^+$.

B. $^{143}Gd^m$ decay

We have constructed a decay scheme for $^{143}Gd^m$ that is presented in Fig. 8. Sixty-one γ-rays deexciting 33 levels were placed, and all intensities are presented in percent per decay. Logft values are calculated as mentioned above, and β-decay feeding intensities assume no third forbidden ground-state feeding. The Q_ε value used here is the same as for $^{143}Gd^g$ decay because we have no direct evidence whether the $11/2^-$ or $1/2^+$ state is the ground state. The systematics of this region suggest that $11/2^-$ lies above the $1/2^+$ state but close to it (within ≈100 keV).

The J^π for ^{143}Eu are based on experimental multipolarities and γ-ray selection rules. All β transitions with $\log ft \le 6.1$ are assumed to be allowed. Some spin assignments are made on the basis of the theoretical arguments given in the discussion; however, all reasonable experimental possibilities are then provided in parentheses. Further details of the specific spin assignments are discussed below.

0-, 271.94-, and 389.47-keV states

These three states represent the three single-particle shell-model states populated by $^{143}Gd^m$ decay. The ground state is the $\pi d_{5/2}$ proton state as was confirmed by

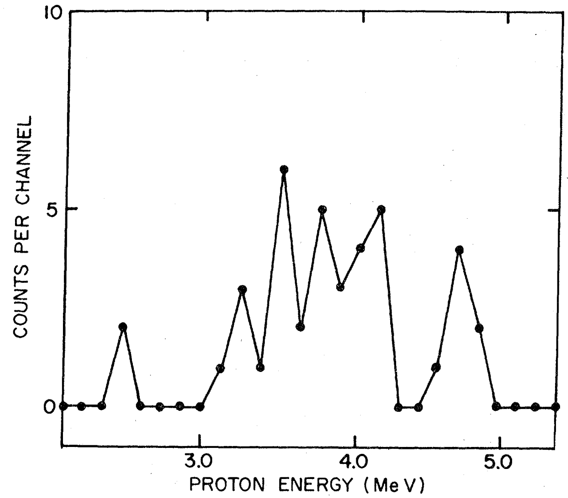

FIG. 6. β-delayed protons following the decay of ^{143}Gd^{g+m}. These data were taken with a particle telescope, and an upper limit of 1×10^{-5} delayed p/α decays per ^{143}Gd decay was set.

studies of ^{143}Eu β decay itself.[13] The state at 271.94 keV is the $\pi g_{7/2}$ proton state as confirmed by the *M*1 γ ray deexciting it to the ground state and the *M*2 γ ray feeding it from the $\pi h_{11/2}$ proton state at 389.47 keV. This $\pi h_{11/2}$ state is further confirmed by its *E*3 transition to the ground state. The 50.0-μsec half-life of the 389.47-keV state made coincidence measurements with γ-rays feeding through this state impractical, so transitions placed into it were generally confirmed by other interlocking coincidence relationships or by β- and γ-decay selection rules, which eliminate direct feeding to the ground state.

906.96-, 2018.8-, 2064.9-, and 2092.1-keV states

These were the only higher-lying states where definite J^π assignments could be made from the experimental data. The 906.96-keV γ from the state of the same energy is known to be *E*2 and the β decay is clearly either allowed or first forbidden, eliminating spins $7/2^+$ or lower. The 906.96-keV state is therefore uniquely determined as $9/2^+$. The β transitions to the states at 2018.8-, 2064.9-, and 2092.1-keV are all allowed, limiting their assignments to $9/2^-$, $11/2^-$, or $13/2^-$. Each of these states deexcites strongly through the $\pi g_{7/2}$ state, leaving only the spin $9/2^-$ assignment.

Other states

The remaining states are not uniquely determined by experiment; however, gener-

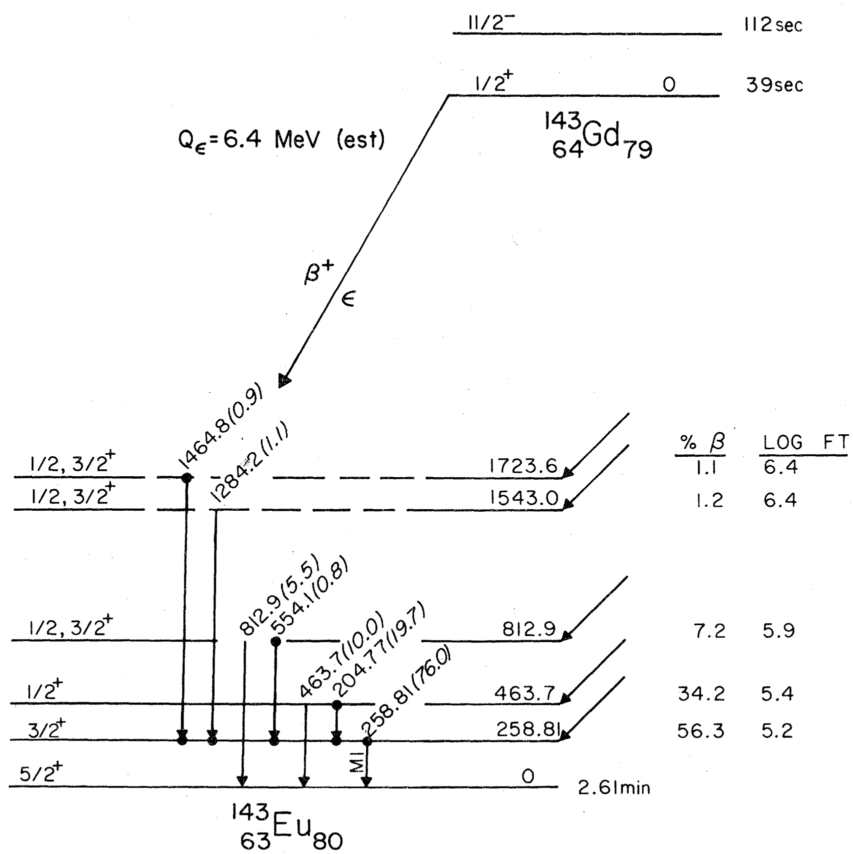

FIG. 7. Decay scheme for ^{143}Gd^g.

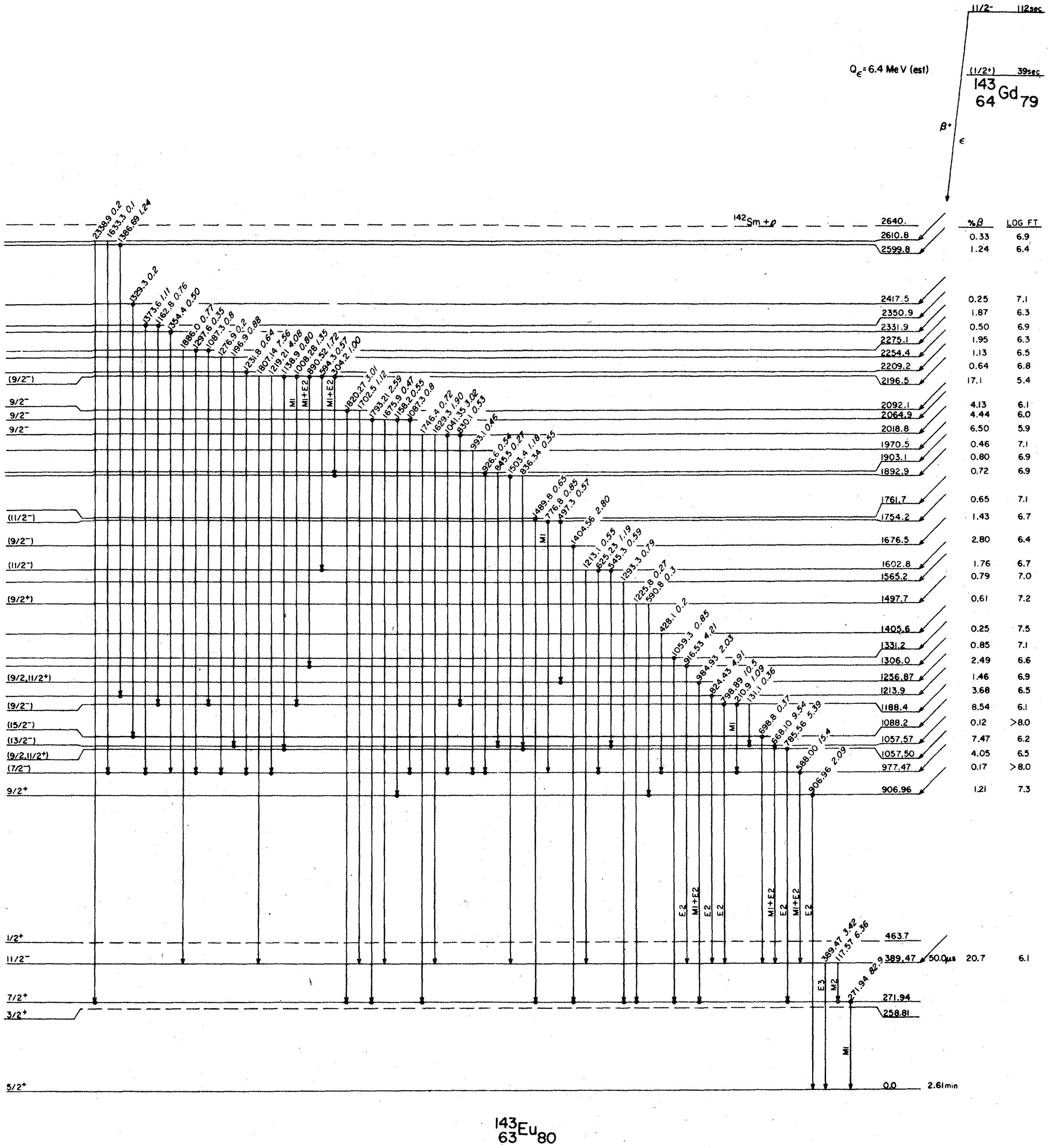

FIG. 8. Decay scheme for $^{143}Gd^{m}$.

ally some spins can be eliminated. Here we have assumed that log$ft \le 6.1$ signifies an allowed β transition, log$ft \le 7.0$ an allowed or first forbidden non-unique transition, and log$ft \ge 7.0$ an allowed, first forbidden, or first forbidden unique transition. The latter limit is somewhat generous; however, we believe that the weak feedings with high logft's cannot be measured with sufficient sensitivity to rule out higher orders of forbiddenness. In addition, γ-ray transitions from these states were expected to follow standard selection rules and to conform to the measured multipolarities. In the cases where $M1$ or $E3$ were indistinguishable in the conversion work, we chose the $M1$, because the $E3$ in each case was highly forbidden with respect to other competing transitions. One exception to these criteria was the 1256.87-

TABLE III. Calculated[a] and experimental[b] conversion coefficients for the 985-keV transition in ^{143}Eu.

MULTIPOLARITY	α_K
*M*1	5.9×10^{-3}
*M*2	1.6×10^{-2}
*E*2	3.4×10^{-3}
*E*3	7.4×10^{-3}
Experiment	$(6.9\pm1.4)\times10^{-3}$

[a]R. S. Hager and E. C. Seltzer, Nucl. Data Tables A4, 1 (1968).

[b]K. Wisshak et al., Z. Physik A277, 129 (1976).

keV state. The 984.93-keV transition from this state was reported to be $M2+E3$, suggesting $J^\pi = 11/2^-$. (Wisshak et al. reported $\alpha_K = (6.9\pm1.4)\times10^{-3}$ and assigned this transition as $M2+E3$.) From Hager and Seltzer[14] we find the values given in Table III for a 985-keV transition. Clearly $M2$ is eliminated and the best assignment for the transition must be $M1+E2$, although $E3$ cannot be eliminated on this basis alone. Additionally, the $M1+E2$ transition through the $\pi h_{11/2}$ state would have to be hindered by over four orders of magnitude with respect to an $M2+E3$ transition for the latter assignment to be viable. We therefore assume that Wisshak et al. were mistaken in their assignment; we prefer $9/2^+$ or $11/2^+$ but cannot rule out $9/2^-$ or $11/2^-$.

One interesting point in our ^{143}Gd^m decay scheme is that we have placed two 1087.3-keV γ transitions; one deexciting the 2064.9-keV level, the other, the 2275.1-keV level. This situation was forced on us because the 1087.3-keV γ is in prompt coincidence with both the 588.00- and 798.89-keV γ's. In addition, the two levels placed by this apparent doublet are confirmed by numerous other transitions. We were unable to resolve the doublet in any spectrum and could set an upper limit of 1 keV on the separation. Coincidence data indicated that the 1087.3-keV γ's also were of nearly equal intensity. There are no other reasonable placements for a 1087.3-keV γ that do not require an additional, unobserved coincident transition. We find this feature of the decay scheme amusing but probably not as uncommon as might first be suspected.

The specific J^π assignments for the higher-lying states are somewhat model dependent and will be discussed in the following section.

V. DISCUSSION

The ^{143}Eu level systematics were discussed by Wisshak et al.[6] using a decoupling model where only the 2_1^+ and 4_1^+ core states were coupled to the $\pi h_{11/2}$ single-particle state to obtain the primary β-fed negative-parity states in ^{143}Eu. In this section we shall show that the assignments made by Wisshak et al. were generally incorrect because of their limited knowl-

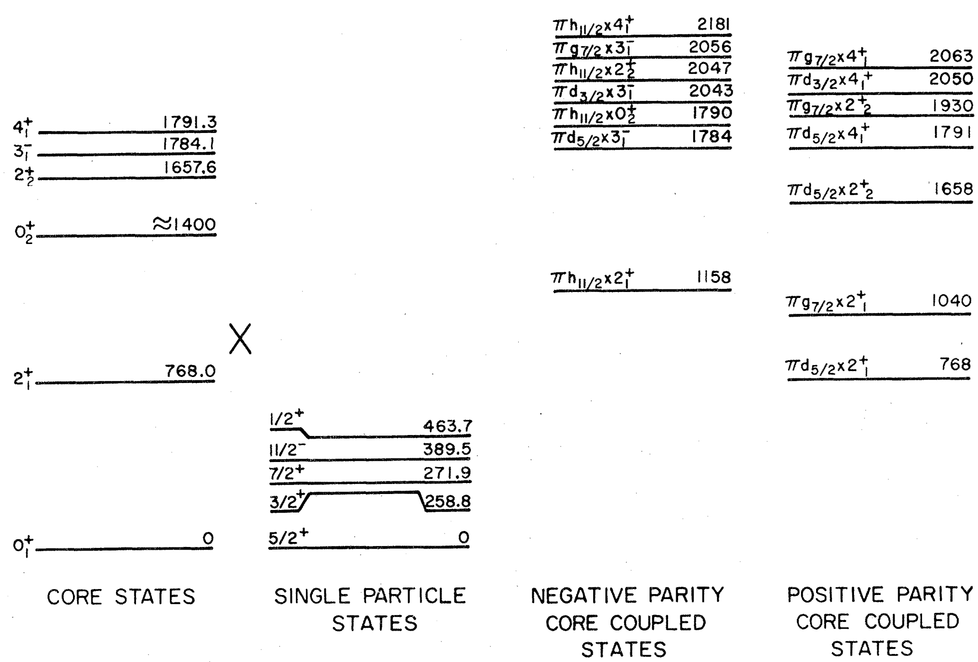

FIG. 9. Single-coupling model for states in ^{143}Eu based on the coupling of the ^{142}Sm core with the low-lying ^{143}Eu single-quasiparticle proton states.

edge of the decay scheme. We now believe that the spin assignments chosen by Wisshak et al. to minimize the χ^2 of their fit were incorrect and the choice $\gamma = 0°$ was too large an asymmetric deformation. We shall discuss ^{143}Eu below in the triaxial weak-coupling model described by Meyer-ter-Vehn.[15] The discussion will include all core states through the 4_1^+ and their coupling to every single-particle level. Meyer-ter-Vehn's quantitative calculations for the $\pi h_{11/2}$ coupling to the 2_1^+, 2_2^+, and 4_1^+ core states will be utilized extensively, and more general qualitative remarks will be made concerning the other single-particle couplings.

The single-particle states discussed here are presumed to couple to the excited states in the ^{142}Sm core. The low-lying states in ^{142}Sm were identified by Kennedy, Gujrathi, and Mark[16] and are displayed in Fig. 9. The low-lying 0_2^+ state was not observed; however, this state appears at 1477.9 keV in ^{138}Ce[17] and at 1413.4 keV in ^{140}Nd.[18] We have assumed that the 0_2^+ state lies at about 1400 keV; however, its exact position is not crucial to this discussion. The 2_1^+ state in ^{142}Sm lies at 768.0 keV, which allows us to predict the deformation parameter $\beta = 0.12$, as pointed out by Grodzins.[19] This value of β is small enough to justify a triaxial weak-coupling model and to predict the relatively small splittings in the predicted core-coupled multiplets. This is certainly true for couplings to the $\pi h_{11/2}$ unique parity state and hopefully at least approximately correct for couplings to the other single-particle states.

The β decay of $^{143}Gd^{g+m}$ must also be consistent with the weak-coupling picture we intend to adopt. The predominant shell-model configuration for protons in $^{143}Gd^{g+m}$ is $(\pi g_{7/2})^8(\pi d_{5/2})^6$. β decay from this configuration to either $\nu h_{11/2}$ or $\nu s_{1/2}$ states are strictly forbidden in the simple shell-model sense, and pairing occupation in the $\pi s_{1/2}$, $\pi d_{3/2}$, and $\pi h_{11/2}$ orbitals in $^{143}Gd^{g+m}$ must be considered to explain the observed decays. In the shell-model picture, this means that we would see decay to numerous three-quasiparticle states in ^{143}Eu (as in the decay of $^{145}Gd^g$[20]), or, in a more general collective picture, to core-coupled states where these core states are essentially two or more quasiparticle combinations.

The model we choose to predict the β decay systematics is the $^{142}Eu^{g+m}$ decay to the same ^{142}Sm core described by Kennedy, Gujrathi, and Mark.[16] With the exception of the $\pi d_{5/2} \rightarrow \nu d_{3/2}$ ground state β transition, the decay to excited states in ^{142}Sm provides us with the expected $\log ft$'s for the β transitions to the core-coupled states in ^{143}Eu. The additional odd proton is weakly coupled to the core and is essentially carried along in ^{143}Gd β decay. The observed $^{142}Eu^g$ decay to the three lowest 2^+ states in ^{142}Sm all have $\log ft \approx 5.2$, and the allowed decay to the 0_2^+ state was unobserved, suggesting a significantly more hindered transition. Also in $^{142}Eu^m$ decay, fast first-forbidden transitions with $\log ft \approx 6.5$ were observed. Thus, we expect ^{143}Gd decay to populate many low-lying $9/2^+$, $11/2^+$, and $13/2^+$ states in ^{143}Eu by observable first-forbidden β transitions. We also expect a Gamow-Teller sum rule such that the total Gamow-Teller strength to a particular core-coupled multiplet yields a net $\log ft$ appropriate to the core state itself. We would additionally expect the distribution of Gamow-Teller strength to follow the $j+1/j$ ($j = \ell+1/2$) or $j/j+1$ ($j = \ell-1/2$) single-particle selection rules for allowed decay to a given negative-parity multiplet. For $h_{11/2}$ particles the ratio of $9/2^-$ to $11/2^-$ to $13/2^-$ reduces to 0.34/0.33/0.32, i.e., roughly equal feedings. These predictions will break down near 2 MeV in ^{143}Eu, where the level density becomes high enough for the levels of a given spin to mix extensively. We should also expect the decay systematics to break down where weak coupling is not so valid, such as the nonunique-parity state couplings.

Single-particle states

The five lowest-lying states in ^{143}Eu are presumed to be described best as the single-quasiparticle shell-model states. They lie at 0 ($\pi d_{5/2}$), 258.81 ($\pi d_{3/2}$), 271.94 ($\pi g_{7/2}$), 389.47 ($\pi h_{11/2}$), and 463.7 keV ($\pi s_{1/2}$). The $\pi h_{11/2}$ state is metastable ($t_{1/2}$ = 50.0 μsec) in analogy with the lighter odd-A N=78 nuclei.

Negative-parity states

The expected core-coupled negative-parity states are also shown in Fig. 9. The low-lying $(\pi h_{11/2} \times 2_1^+)$ states should be rather pure configurations. They may be identified by their $E2$ transitions through the $\pi h_{11/2}$ single-particle state, $M1 + E2$ transitions among themselves, and fast allowed β transitions of roughly equal strength from $^{143}Gd^m$ to the $9/2^-$, $11/2^-$, and $13/2^-$ members. The $7/2^-$ and $15/2^-$ states will not be seen by direct β feeding; however, they may be observed by γ-ray branchings. The levels corresponding to $(\pi h_{11/2} \times 2_1^+)$ should be observed at about 1158 keV in ^{143}Eu.

Two relatively fast β transitions occur to the states at 1057.57 and 1188.4 keV. The 1188.4- and 1602.8-keV states both deexcite through the 1057.57- and 977.47-keV states. These states all deexcite through the $\pi h_{11/2}$ state and may represent four of the states in the $(\pi h_{11/2} \times 2_1^+)$ multiplet.

The 977.47-keV state is not fed directly by β decay, and feeding from higher-lying $9/2^-$ states suggests that this state might be the $(\pi h_{11/2} \times 2_1^+)_{7/2^-}$ component. The $M1$ transition from the 1188.4- to the 977.47-keV state then suggests that the $(\pi h_{11/2} \times 2_1^+)_{9/2^-}$ configuration lies at 1188.4 keV. The 1602.8-keV state feeds the 977.47-keV state, forcing the $(\pi h_{11/2} \times 2_1^+)_{11/2^-}$ assignment and leaving the $(\pi h_{11/2} \times 2_1^+)_{13/2^-}$ assignment for the 1057.57-keV state.

A state at 1088.2 keV is observed to deexcite through the $\pi h_{11/2}$ state and has no direct β feeding. This state is tentatively assigned as the $(\pi h_{11/2}\times 2_1^+)_{15/2^-}$ configuration. We might expect this state to be populated by γ decay from the $(\pi h_{11/2}\times 2_1^+)_{11/2^-}$ state, however the expected 514.6-keV γ would be masked by the strong $\gamma^{\pm}$ radiation. The lack of feeding from the strongly fed $9/2^-$ states at 2 MeV also tends to corroborate this assignment.

The allowed β decay is observed to proceed roughly equally to the $9/2^-$ and $13/2^-$ states; however, the $11/2^-$ component is fed by only 50% of the Gamow-Teller strength to the others. This discrepancy is probably explained by the unobserved 514.6-keV transition and the significant mixing of this state with the nearby $(\pi h_{11/2}\times 0_2^+)_{11/2^-}$ and $(\pi d_{5/2}\times 3_1^-)_{11/2^-}$ states. The net log*ft* to these five states is observed to be 5.4, and if we assume the total strength to the $11/2^-$ is equal to that of the others, this reduces to a net log*ft* of 5.2, which is in excellent agreement with our earlier prediction from ^{142}Eu^g decay.

From Meyer-ter-Vehn's calculations for $\gamma_F = \epsilon_1$,[15] we can read from his graph that for $E_{2^+} = 768$ keV, the $(\pi h_{11/2}\times 2_1^+)_{7/2^-}$ component should lie lowest, the $9/2^-$, $13/2^-$, and $15/2^-$ components should all lie close together at ≈130 keV above this, and the $11/2^-$ component should lie at 490 keV above the $7/2^-$ state. The agreement with theory is remarkable, both in the level ordering and the energy separations.

The $(\pi h_{11/2}\times 0_2^+)_{11/2^-}$ state is not so readily identifiable and should presumably lie near 1800 keV in ^{143}Eu. It should deexcite through 2_1^+-coupled states and perhaps avoid deexciting strongly through single-particle states. Unfortunately, mixing with nearby $11/2^-$ states will cloud the issue. The best candidate is probably the state at 1754.2 keV; however, this can only be a tentative assignment.

The $(\pi d_{5/2}\times 3_1^-)_{9/2^-,11/2^-}$ states are nominally expected near 1784 keV in ^{143}Eu. The best candidates for the $9/2^-$ state lie at 1676.5 and 2064.9 keV. The lower state is close to the correct energy, and selection rules limit it to spin $9/2^-$ if it is of negative parity. The upper state is weakly favored because of its deexcitation through the $(\pi d_{5/2}\times 2_1^+)_{9/2^+}$ state, which will be discussed in detail below. If the $11/2^-$ component lies low, it will probably be either the 1213.9- or 1306.0-keV state, both of which are moderately strongly β fed, and if they were $11/2^-$ could only deexcite through the $\pi h_{11/2}$ single-particle state.

The $(\pi h_{11/2}\times 2_2^+)_{9/2^-,11/2^-,13/2^-}$ states are expected to lie near 2047 keV. The calculations of Meyer-ter-Vehn suggest that the $11/2^-$ and $13/2^-$ components should occur 200-300 keV higher, where the level density becomes much greater, so that these levels will become extensively mixed. The $9/2^-$ strength is therefore likely to be primarily in the strongly-fed triplet of $9/2^-$ states at about 2 MeV. A similar splitting is calculated for the $(\pi h_{11/2}\times 4_1^+)_{9/2^-,11/2^-,13/2^-}$ states at 2181 keV, suggesting the state at 2196.5 keV is also $9/2^-$; however, we might then expect this state to feed the $\pi g_{7/2}$ state at least weakly. Nevertheless, we see deexcitation of the 2196.5-keV state to numerous 2_1^+ coupled states, as would be expected from a $(\pi h_{11/2}\times 4_1^+)$ configuration. Other $9/2^-$ states will arise from $(\pi d_{3/2}\times 3_1^-)$ at about 2043 keV and $(\pi g_{7/2}\times 3_1^-)$ at about 2056 keV. These five $9/2^-$ states near 2 MeV may be strongly mixed with one another and additionally are most likely mixed with the 1676.5-, 2018.8-, 2064.9-, 2092.1-, and 2196.5-keV states. The $11/2^-$ and $13/2^-$ members of these configurations may include the 1213.9- or 1306.0-keV low-lying states and the numerous well mixed states above 2 MeV, where they cannot be directly identified.

Positive-parity states

The expected low-lying positive-parity states in ^{143}Eu are again shown in Fig. 9. These states are all expected to give poorer (not so simple) weak-coupling descriptions, and we are not aware of specific calculations for these states. The assignments of the positive-parity states below to the weak coupling system will be made primarily on the basis of the excitation energy and the decay systematics of these states. All first-forbidden transitions to low-lying states are expected to be observable, and some first-forbidden-unique transitions may also be seen.

The $(\pi d_{5/2}\times 2_1^+)$ states should lie at ≈768 keV in ^{143}Eu. They should deexcite strongly to the $\pi d_{5/2}$ ground state by $E2(+M1)$ transitions. The state at 906.96 keV is probably the $(\pi d_{5/2}\times 2_1^+)_{9/2^+}$ component, and either the $1/2^+$ or $3/2^+$ member is seen at 812.9 keV. A third member should be seen from ^{143}Gd^g decay; however, ^{143}Gd^g apparently feeds it too weakly to identify it in these experiments. If the 812.9-keV state is $1/2^+$, we expect ≈64% of the β decay to feed this state directly. Assuming the remainder goes to the unobserved $3/2^+$ member, the net log*ft* to $(\pi d_{5/2}\times 2_1^+)_{1/2^+,3/2^+}$ is 5.5, a bit large compared to our predictions for ^{142}Eu^g decay but perhaps consistent with a partial breakdown of the weak-coupling model for this state.

The $(\pi g_{7/2}\times 2_1^+)$ couplings lead to observable $9/2^+$ and $11/2^+$ states in the vicinity of 1040 keV which should be fed by ^{143}Gd^m decay. These states should deexcite through the $\pi g_{7/2}$ single-particle state by strong $E2$ transitions. The most likely candidates lie at 1057.50 and 1256.87 keV, although no final assignments can be made from these data. The log*ft*'s of 6.5 and 6.9, respectively, are consistent with such first-forbidden assignments. The $(\pi g_{7/2}\times 2_1^+)_{3/2^+}$ state should also be seen from ^{143}Gd^g decay, although it may mix strongly with nearby states. No such state is observed experimentally.

The $(\pi d_{5/2}\times 2_2^+)_{9/2^+}$ state is expected to be observed at ≈1658 keV. It should deexcite strongly to the $(\pi d_{5/2}\times 2_1^+)_{9/2^+}$ state, although it may mix strongly with neighboring $9/2^+$ states. The most likely candidate lies at 1497.7 keV. The logft = 7.2 for β decay to this state is similar to that for the 906.96-keV state (7.3), as would be expected. The $(\pi d_{5/2}\times 2_2^+)_{1/2^+,3/2^+}$ states might be the ones observed at 1543.0 and 1723.6 keV; however, these states must surely be mixed strongly with the nearby states. The logft = 5.8 for β decay to these states is comparable to that for the lower-lying $(\pi d_{5/2}\times 2_1^+)$ configurations; however, little significance can be put on this result at this time.

Numerous other positive-parity couplings below 2 MeV can be suggested as shown in Fig. 9, and certainly most such states are observed in $^{143}Gd^m$ decay. No further attempts will be made to predict which states are composed of which principal components; however, approximately the correct number of states are observed to correspond to the weak-coupling predictions.

Conclusions

The weak-coupling model has been shown to give an excellent qualitative understanding of the low-lying level structure in ^{143}Eu. The $(\pi h_{11/2}\times 2_1^+)$ quintet appears in its entirety and offers excellent quantitative agreement with the predictions of Meyer-ter-Vehn. The low-lying positive-parity states and the multiplet of $9/2^-$ states at ≈2 MeV are also well reproduced. Weak coupling seems to be at least approximately valid for the nonunique-parity level couplings, and the β decay systematics fit quite nicely with these general arguments. Although more detailed calculations might in some instances prove helpful, it is still most desirable to identify the remaining members of the partially identified multiplets. To this end ^{144}Sm(p,2$n\gamma$)^{143}Eu in-beam experiments are planned by these authors in the near future.

ACKNOWLEDGEMENTS

The authors wish to acknowledge the helpful discussions relevant to the theoretical section of this paper with Dr. B. A. Brown and Dr. T. L. Khoo of the MSU Cyclotron Laboratory

---

*Work supported in part by the National Science Foundation.

[1]D. B. Beery, Ph.D. Thesis, Michigan State University (1969).
[2]D. B. Beery, W. H. Kelly, and Wm. C. McHarris, Phys. Rev. 188, 1851 (1969).
[3]R. E. Eppley, R. R. Todd, Wm. C. McHarris, and W. H. Kelly, Phys. Rev. C 5, 1084 (1972).
[4]R. R. Todd, Ph.D. Thesis (1971); R. E. Eppley, Ph.D. Thesis, Michigan State University, COO-1779-32 (1970).
[5]J. van Klinken, D. Habs, H. Klewe-Nebenius, K. Wisshak, G. Nowicki, J. Buschmann, S. Göring, R. Löhken, H. Rebel, and G. Schatz, Gesellschaft für Kernforschung mbH KFK 1768 (1973).
[6]K. Wisshak, A. Hanser, H. Klewe-Nebenius, J. Buschmann, H. Rebel, H. Foust, H. Toki, and A. Fässler, Z. Phys. A 277, 129 (1976).
[7]K. L. Kosanke, M. D. Edmiston, R. A. Warner, R. B. Firestone, Wm. C. McHarris, and W. H. Kelly, Nucl. Instr. Meth. 124, 365 (1975).
[8]R. B. Firestone, R. A. Warner, Wm. C. McHarris, and W. H. Kelly, to be published.
[9]I.a., G. C. Giesler, K. L. Kosanke, R. A. Warner, Wm. C. McHarris, and W. H. Kelly, Nucl. Instr. Meth. 93, 211 (1971).
[10]D. Ekström, S. Ingleman, M. Olsmats, and B. Wannberg, Phys. Scr. 6, 181 (1972).
[11]N. B. Gove and M. J. Martin, Nucl. Data Tables A10, 205 (1971).
[12]A. H. Wapstra and K. Bos, Atom. Nucl. Data Tables 17, 474 (1976).
[13]R. B. Firestone, R. A. Warner, Wm. C. McHarris, and W. H. Kelly, to be published.
[14]R. S. Hager and E. C. Seltzer, Nucl. Data Tables A4, 1 (1968).
[15]J. Meyer-ter-Vehn, Nucl. Phys. A249, 111 (1975).
[16]G. G. Kennedy, S. C. Gujrathi, and S. K. Mark, Phys. Rev. C 12, 553 (1975).
[17]G. M. Julian and T. E. Fessler, Phys. Rev. C 3, 751 (1971).
[18]G. G. Kennedy, S. C. Gujrathi, and S. K. Mark, Z. Phys. A274, 233 (1975).
[19]L. Grodzins, Phys. Letters 2, 88 (1962).
[20]R. E. Eppley, Wm. C. McHarris, and W. H. Kelly, Phys. Rev. C 3, 282 (1971).
[21]M. Blann and F. Plasil, nuclear evaporation code ALICE adapted for the MSU Cyclotron Laboratory Sigma-7 computer by W. Bentley.